

1992

# Pressure Pulsation in Hermetic Casing of Refrigerating Rotary Compressor

T. Yanagisawa  
*Shizuoka University; Japan*

T. Shimizu  
*Shizuoka University; Japan*

M. Fukuta  
*Shizuoka University; Japan*

M. Ueda  
*Shizuoka University; Japan*

Follow this and additional works at: <https://docs.lib.purdue.edu/icec>

---

Yanagisawa, T.; Shimizu, T.; Fukuta, M.; and Ueda, M., "Pressure Pulsation in Hermetic Casing of Refrigerating Rotary Compressor" (1992). *International Compressor Engineering Conference*. Paper 866.  
<https://docs.lib.purdue.edu/icec/866>

This document has been made available through Purdue e-Pubs, a service of the Purdue University Libraries. Please contact [epubs@purdue.edu](mailto:epubs@purdue.edu) for additional information.

Complete proceedings may be acquired in print and on CD-ROM directly from the Ray W. Herrick Laboratories at <https://engineering.purdue.edu/Herrick/Events/orderlit.html>

# PRESSURE PULSATION IN HERMETIC CASING OF REFRIGERATING ROTARY COMPRESSOR

Tadashi YANAGISAWA, Associate professor  
Takashi SHIMIZU, Professor  
Mitsuhiro FUKUTA, Research Associate  
Motohiko UEDA, Graduate Student

Department of Energy and Mechanical Engineering,  
Shizuoka University,  
3-5-1, Johoku, Hamamatsu, 432, JAPAN

## ABSTRACT

In this study, a discharge flow path of a refrigerating rotary compressor is modeled by a piping system which consists of three pipes (a cylinder passage, a motor passage and a discharge pipe) and three volumes (a valve chamber, chambers over and under a motor in a hermetic casing), and pressure pulsation in the piping system is analyzed theoretically by transfer matrix method. Theoretical calculation indicates that intermittent discharge flow from a cylinder causes certain pressure pulsation in both upper and lower chambers in the casing, and the theoretical pressure pulsation is in good correlation with experimental one in phase and amplitude of the pulsation. It is also confirmed theoretically and experimentally that the pressure pulsation in the chambers over and under the motor induces a longitudinal vibration of a motor rotor.

## NOMENCLATURE

a : sound velocity  
C : damping coefficient of vibration  
c : coefficient of discharge at valve port  
F : magnetic thrust force of motor  
g : acceleration of gravity  
k : adiabatic compression exponent  
m : mass of rotor including shaft mass  
P : pressure  
 $Q_v$  : discharge flow rate through valve port  
S : sectional area of pipe  
 $S_r$  : sectional area of rotor  
 $S_v$  : area of valve port  
t : time  
U : flow rate  
V : volume  
X : longitudinal displacement of rotor  
z : distance along pipe  
 $\rho$  : density  
u : damping coefficient of flow oscillation

### Subscript

c : compression chamber in cylinder  
1 : valve chamber  
2 : lower chamber in casing  
3 : upper chamber in casing

### Superscript

\* : component of fluctuation

## INTRODUCTION

This study investigates pressure pulsation in a discharge flow path of a refrigerating rotary compressor which is enclosed in a hermetic casing with discharge pressure.

There have been many studies / (1)-(4) / on pressure pulsation in suction and discharge flow paths of reciprocating compressors for refrigerating use. Concerning refrigerating hermetic rotary compressors, some studies / (5)-(7) / investigated pressure pulsation in a suction path of the compressor because the suction pressure pulsation is larger than pressure pulsation in a discharge path including large volume in the hermetic casing and is more influential on capacity of the compressor.

In recent years, however, with increasing rotational speed of the compressor driven by an inverter, the discharge pressure pulsation becomes serious and in the worst case it may induce longitudinal vibration of a motor rotor in the casing. This study analyzes theoretically and experimentally the discharge pressure pulsation in the hermetic casing of the rotary compressor and investigates liability of the flow-induced vibration of the rotor.

## THEORETICAL ANALYSIS

### Model of Discharge Flow Path

Figure 1 shows a schematic view of a rolling piston type rotary compressor which is analyzed in this study. A compression mechanism and an induction motor are set in a hermetic casing. Suction refrigerant is compressed in a cylinder and is delivered through a discharge valve into a valve chamber. The refrigerant flows into a chamber under the motor in the casing through a cylinder passage and reaches a lower chamber in the casing through a motor passage, then it flows out from the compressor through a discharge pipe.

The discharge flow path of the rotary compressor is modeled by a piping system shown in Figure 2 which consists of three pipes (pipe 1: the cylinder passage, pipe 2: the motor passage, pipe 3: the discharge pipe) and three volumes (volume 1: the discharge valve chamber, volume 2: the lower chamber in the casing, volume 3: the upper chamber in the casing).

### Analysis of Pressure Pulsation

In Figure 2, flow condition in pipes is governed by the following equations:

$$\partial U^* / \partial t + \mu U^* + (S/\rho)(\partial P^* / \partial z) = 0 \quad (1)$$

$$\partial P^* / \partial t = -(\rho a^2 / S)(\partial U^* / \partial z) \quad (2)$$

where,  $U$ : volumetric flow velocity,  $P$ : pressure,  $\rho$ : density,  $S$ : sectional area of pipe,  $a$ : sound velocity,  $\mu$ : damping coefficient of flow oscillation,  $t$ : time,  $z$ : distance along pipe, and superscript \* indicates component of fluctuation.

On the other hand, pressure in volumes is governed by the following equation of continuity;

$$dP^* / dt = \rho a^2 (U_{in}^* - U_{out}^*) / V \quad (3)$$

where,  $V$ : volume, and subscripts 'in' and 'out' indicate flowing into the volume and flowing out from the volume.

Based on the above governing equations, pressure pulsation in the piping system is analyzed theoretically by using a transfer matrix method / (8),(9) /. As boundary conditions of the piping system shown in Figure 2, constant pressure is assumed at an end of the discharge pipe (pipe 3). On the other hand, flow rate,  $Q_v$ , entering the valve chamber (volume 1) through the discharge valve port is given by the following equation;

$$Q_v = \left\{ \begin{array}{l} c S_v \sqrt{2k/(k-1)} \{P_c / \rho_c\} \left\{ 1 - (P_1 / P_c)^{(1-1/k)} \right\} \quad (P_c > P_1) \\ 0 \quad (P_c \leq P_1) \end{array} \right\} \quad (4)$$

where,  $P_1$ : pressure in the valve chamber,  $P_c$ : pressure in a compression chamber in the cylinder,  $S_v$ : flow area of the valve port,  $c$ : coefficient of discharge,  $\rho_c$ : density in the compression chamber,  $k$ : adiabatic compression exponent. The pressure,  $P_c$ , in the compression chamber is decided by the following equation by taking account of volume

change,  $dV_c/dt$ , of the compression chamber and the discharge flow rate,  $Q_v$ .

$$dP_c/dt = - (kP_c/V_c)(dV_c/dt + Q_v) \quad (5)$$

An example of the intermittent discharge flow rate,  $Q_v$ , calculated for an experimental compressor described later is shown in Figure 3 with rotational speed,  $N$ , as a parameter. The flow rate is approximated with Fourier series and is given as the boundary condition at the valve port.

### Analysis of Flow-induced Vibration of Rotor

In the casing of the compressor, pressures in chambers over and under the motor are different from each other, which may cause longitudinal displacement of the motor rotor when the pressure differential force is larger than self-weight of the rotor. The longitudinal motion of the rotor shown in Figure 4 is expressed by the following equation;

$$m d^2 X/dt^2 = \Delta P S_r - mg - C dX/dt - F \quad (6)$$

where,  $m$ : mass of the rotor including mass of the shaft,  $X$ : displacement,  $\Delta P$ : differential pressure ( $=P_2 - P_3$ ),  $S_r$ : sectional area of the rotor,  $g$ : acceleration of gravity,  $C$ : damping coefficient of vibration,  $F$ : magnetic thrust force of the motor due to a skew of the rotor and due to assembling inaccuracy of the motor. Equation (6) is integrated numerically within a range of longitudinal play of a shaft thrust in the cylinder.

## EXPERIMENT

As shown in the former Figure 1, the experimental rotary compressor is equipped with piezo electric type pressure transducers to measure pressure pulsation in the upper and lower chambers in the casing and is also equipped with an eddy current type displacement sensor to detect longitudinal displacement of a disc fixed on the rotor top.

The compressor is connected to an experimental refrigeration cycle using R22 as a working fluid and is operated under a steady state condition (suction and discharge pressures: 0.49 and 1.96 MPa [gauge], discharge temperature: 90 °C, rotational speed: 40 to 130 1/s). At that time, signals of the pressure transducers and the displacement sensor are recorded with a personal computer via an A/D converter. After the measurement, the compressor is stopped and is started up again under a blocked suction (no suction) condition in order to obtain a reference signal of the displacement sensor under no discharge flow condition.

Main dimensions of the experimental compressor are displacement: 20.7 cm<sup>3</sup>/rev, volume of valve chamber: 55 cm<sup>3</sup>, volume of lower chamber: 350 cm<sup>3</sup>, volume of upper chamber: 470 cm<sup>3</sup>, diameter of valve port: 9 mm, length and sectional area of cylinder passage: 47 mm and 72 mm<sup>2</sup>, length and sectional area of motor passage: 90 mm and 540 mm<sup>2</sup>, length and sectional area of discharge pipe: 2000 mm and 44 mm<sup>2</sup>, coefficient of discharge at valve port: 0.6, mass of rotor including shaft mass: 1.9 kg, diameter of rotor: 60 mm, longitudinal play of shaft thrust: 0.2 mm, magnetic thrust force: 10 N.

## RESULTS AND DISCUSSION

### Experimental Results

Figure 5 shows experimental results of pressure pulsation in the casing and signals of the rotor displacement sensor at different rotational speed,  $N$ . Abscissa of the figure is expressed by rotational angle of the shaft for four cycles of the rotation with a compression starting point as a reference angle. Concerning the pressure curves, broken and solid lines indicate pressures in the upper and lower chamber of the casing respectively, and they are drawn in the way that average of each pressure curve becomes zero. When the rotational speed is low, the pressures pulsate more than one per one revolution though the intermittent discharge flow from the cylinder occurs one per one revolution. Phase of the pulsation of the upper chamber pressure is later than that of the lower chamber pressure, and amplitude of the former is somewhat larger than that of the latter. With increasing the rotational speed, number

of the pulsation per one revolution decreases, and phase lag and amplitude of the pulsating pressure become large. In the experiments, average pressures in the upper and lower chambers were additionally measured with strain gauge type pressure transducers. Difference of the average pressures was no more than 1 kPa and was much less than magnitude of the pulsation amplitude.

Concerning signals of the displacement sensor in Figure 5, a solid line indicate the sensor output measured under the steady state operating condition of the compressor and a dotted line indicates the sensor output under the no flow condition. The curves include large periodic change due to inclination of the displacement disc fixed on the rotor and also include small peak due to a rotational angle marker on the disc. Real longitudinal lift of the rotor is evaluated by the difference of the solid and dotted lines, and it will be illustrated in the later Figure 8.

### Comparison of Theoretical and Experimental Results

Figure 6 shows influence of the damping coefficient of flow oscillation,  $\mu$ , on the theoretical pressure pulsation in the case that the rotational speed is 60 1/s. At the figure, ordinates  $P_2$  and  $P_3$  indicate pressures in the lower and upper chambers. Solid, broken and dotted lines correspond to  $\mu=0, 100, 1000$  1/s respectively. With increasing the value of the coefficient, amplitude of the pressure pulsation becomes small.

There have been some investigations [(10),(11)] on the value of the flow damping coefficient, but their results cannot be applied directly to this study because cross section of the motor passage is not a circular but a complicated shape and because working fluid includes many droplets of oil. In this study, hence, the theoretical calculation is executed for various values of the damping coefficient, which are constant not depending on the compressor speed or change, in proportion to the compressor speed or change in proportion to square root of the speed, and effectiveness of the calculated results is examined by comparison with experimental results.

Figure 7 shows theoretical results which are calculated with appropriate values of the damping coefficient which is in proportion to square root of the compressor rotational speed,  $N$ . As a whole, the results agree well with experimental results in phase and amplitude of the pulsation. In addition, according to the theoretical calculation in wider compressor operating speed, natural frequency of the discharge piping system of the experimental compressor is 163 Hz. As the compressor speed approaches the natural frequency, amplitude of the pressure pulsation becomes large.

As examined above, the theoretical method described in this paper is effective to predict pressure pulsation in the compressor casing though further investigation is necessary to select the appropriate value of the flow damping coefficient.

### Flow-induced Vibration of Rotor

Figure 8 shows theoretical and experimental results of the rotor lift and the pressure difference between the lower chamber pressure  $P_2$  and the upper chamber pressure  $P_3$ . The pressure difference is estimated on such assumption that average pressures in the both chambers are equal to each other, and the difference occurs based on the phase difference of the pressure pulsation in the both chambers. The theoretical pressure difference shown by a broken line is in good correlation with the experimental one shown by a solid line.

On the other hand, the experimental rotor lift is drawn by a solid line and the theoretical lift which changes with value of the damping coefficient of vibration,  $C$ , is drawn by a broken line ( $C=2500$  kg/s) and a dotted line ( $C=0$ ). The former value,  $C=2500$  kg/s, is so selected that the theoretical lift curves agree well with the experimental curves. As shown in Figure 8, with increasing rotational speed of the compressor, the pressure difference increases and lifting of the rotor occurs, and the tendency can be seen in both theoretical and experimental results.

By the way, concerning damping force of the vibration, squeeze force of oil film on the shaft thrust is superior to shearing force of oil film on the shaft journal. The damping force equivalent to the coefficient value  $C=2500$  kg/s can easily occur on the thrust though the force changes with thickness of the oil film expected on the thrust.

From the above consideration, it is confirmed that the pressure differential force which occurs by the phase difference of the pressure pulsation in the upper and lower chambers in the casing can be a reason of the longitudinal vibration of the rotor. In design of the discharge path of the rotary compressor, hence, it is needed to pay attention not only to conventional characteristics of oil separation in the casing but also to characteristics of the pressure pulsation in the casing and the flow-induced vibration of the rotor.

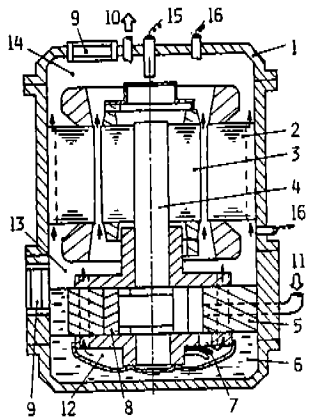
## CONCLUSIONS

Pressure pulsation in the hermetic casing of the rolling piston type rotary compressor was investigated theoretically and experimentally. Certain pressure pulsation in the chambers over and under the motor in the casing was induced by the intermittent discharge flow from the cylinder. The experimental pulsation can be estimated theoretically by the model of the piping system which consists of three pipes and three volumes. It was also confirmed that the pressure pulsation could be a cause of the longitudinal vibration of the rotor.

In the theoretical analyses of the pressure pulsation and the flow-induced vibration of the rotor, damping coefficients of flow oscillation and vibration are used and further investigation on the values of these coefficients is needed.

## REFERENCES

- (1) Sinji, Y. and Nozawa, S., "Effect of Pressure Pulsation on the Performance of Reciprocating Compressors in Refrigerators". Refrigeration (in Japanese), 48-547 (1973), 403.
- (2) Sungh, R. and Nieter, J. J., "An Analytical Relationship between Compressor thermofluid Efficiency and Manifold Acoustic Modes", Proc. 1984 Int. Compr. Eng. Conf., (1984-7), 418.
- (3) Farstad, J. E. and Singh, R., "An Acoustic Transfer Matrix Model for Compressor and Condenser Interaction", Proc. 1990 Int. Compr. Eng. Conf., (1990-7), 362.
- (4) Kim, J. and Soedel, W., "Convergence of Gas Pulsation Simulations When Combining Time and Frequency Domains Iteratively", Proc. 1990 Int. Compr. Eng. Conf., (1990-7), 641.
- (5) Yanagisawa, T. and Shimizu, T., "Influence of Suction Piping on Performance of Rotary Compressor", Proc. 1980 JAR Annu. Conf. (in Japanese). (1980-11), 103.
- (6) Hirano, H., "Analysis of Suction Passage Loss in a Rotary Compressor", Proc. 1984 Int. Compr. Eng. Conf., (1984-7), 427.
- (7) Kakuda, M., Kitora, Y., Hirahara, T. and Yamamoto, T., "Investigation of Pressure Pulsation in Suction Pipe on Rotary Compressor", Proc. 1988 Int. Compr. Eng. Conf., (1988-7), 591.
- (8) Abe, T., Fujikawa, T. and Ito, S., "A Calculation Method of Pulsations in a Piping System", Trans. JSME (in Japanese), 35-277 (1969), 1910.
- (9) Munakata, T., Ohba, M., Toyoda, T. and Wada, H., "Analyses and Experiments of Gas Pressure Pulsations in the Reciprocating Compressor Piping Systems", Ishikawajima Harima Engineering Review (in Japanese), 15-3 (1975), 311.
- (10) Binder, R. C., "The Damping of Large Amplitude Vibrations of a Fluid in a Pipe", J. Acous. Soc. Am., 15-1 (1943), 41.
- (11) Hayama, S., Mohri, Y. and Watanabe, T., "Resonant Amplitudes of Pressure Pulsation in Piping System", Trans. JSME (in Japanese), 42-364 (1976), 3825.



- 1: Casing
- 2: Stator
- 3: Rotor
- 4: Shaft
- 5: Cylinder
- 6: Oil
- 7: Valve
- 8: R. piston
- 9: Sight glass
- 10: Disch. pipe
- 11: Suction pipe
- 12: Valve chamber
- 13: Lower chamber
- 14: Upper chamber
- 15: Gap sensor
- 16: Press. sensor

Figure 1 Schematic view of rotary compressor

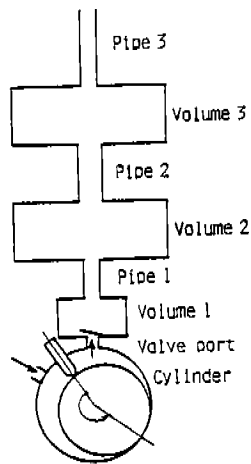


Figure 2 Model of discharge piping system

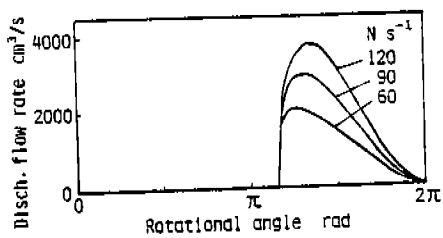


Figure 3 Discharge flow rate

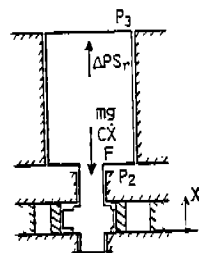


Figure 4 Model of rotor vibration

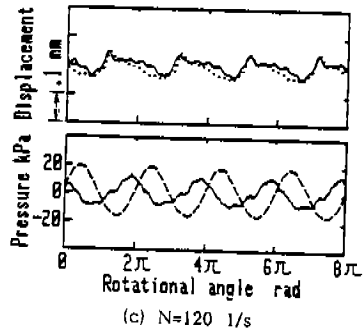
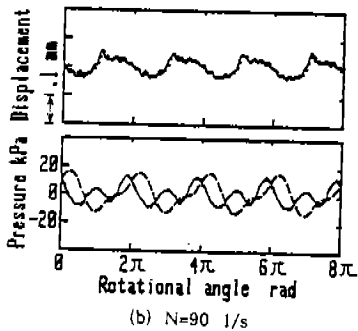
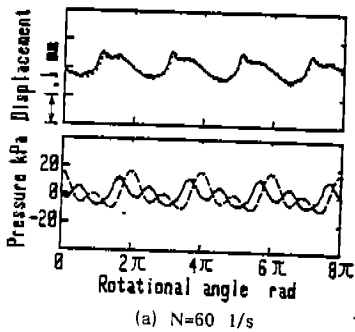


Figure 5 Experimental results. Pressure: —; lower chamber, ----; upper chamber. Displacement: —; steady state condition, .....; no flow condition

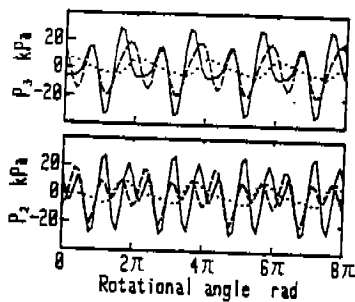


Figure 6 Influence of damping coefficient of flow oscillation,  $\mu$ . —;  $\mu=0$  1/s, ----;  $\mu=100$  1/s, .....;  $\mu=1000$  1/s



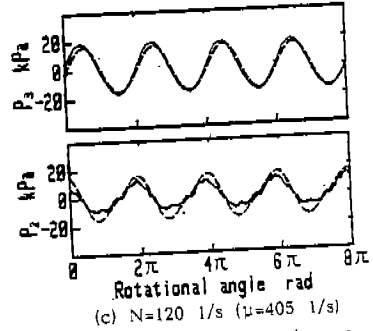
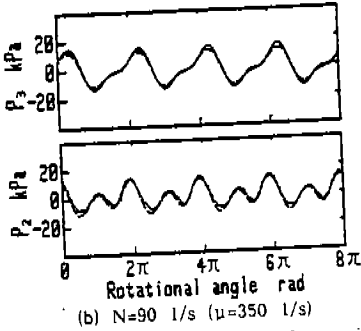
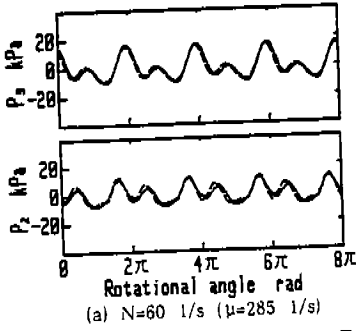


Figure 7 Comparison of experimental and theoretical pressure pulsation.  
 —; measured, - - -; calculated

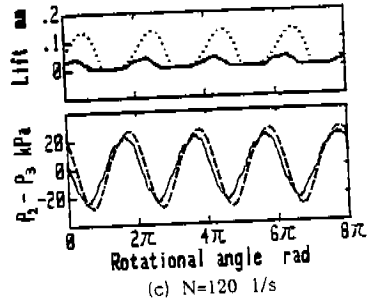
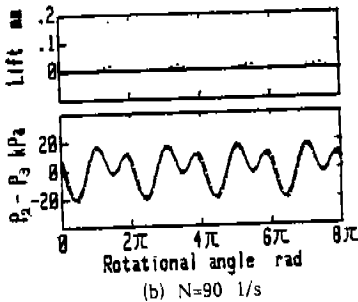
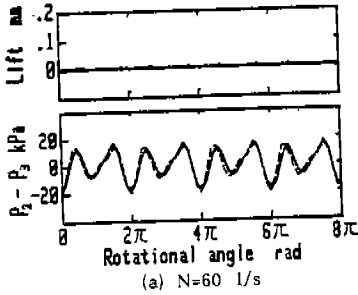


Figure 8 Comparison of pressure difference ( $P_2 - P_3$ ) and rotor lift. —; measured, - - -; calculated ( $C=2500$  kg/s), ·····; calculated lift without damping ( $C=0$ )